International Journal of Thermophysics, Vol. 17, No. 6, 1996

A Nonlinear Regression Analysis for Estimating Low-Temperature Vapor Pressures and Enthalpies of Vaporization Applied to Refrigerants

R. Tillner-Roth[1,2]

Received February 2, 1996

A new method is presented to extrapolate experimental vapor pressures down to the triple point. The method involves a nonlinear regression analysis based on the Clausius–Clapeyron equation and a simple relation for the enthalpy of vaporization. Triple-point pressures and vapor pressures up to 0.1–0.2 MPa are estimated for R125, R32, R143a, R134a, R152a, R123, R124, and ammonia; they generally agree with available experimental data within their uncertainty. Equations for the enthalpy of vaporization which describe this property fairly well at low temperatures are obtained as a byproduct.

KEY WORDS: ammonia; enthalpy of vaporization; extrapolation; R123; R124; R125; R134a; R143a; R152a; R32; refrigerants; triple point; vapor pressure.

1. INTRODUCTION

Vapor-pressure measurements are essential for establishing accurate equations of state. Although this property is usually investigated intensively, there is often a lack of reliable vapor-pressure measurements for temperatures below the normal boiling point.

Generally, the vapor pressure can be estimated from the enthalpy of vaporization Δh_v and the saturated liquid and vapor volumes v' and v'' by integrating the Clausius–Clapeyron equation,

$$T\frac{dp_s}{dT}=\frac{\Delta h_v(T)}{v''(T)-v'(T)} \tag{1}$$

[1] Thermophysics Division, National Institute of Standards and Technology, 325 Broadway, Boulder, Colorado 80303, U.S.A.

[2] Permanent affiliation: Institut für Thermodynamik, Universität Hannover, Callinstrasse 36, 30167 Hannover, Germany.

0195-928X/96/1100-1365$09.50/0

However, enthalpy of vaporization data are very scarce and such an estimation of vapor pressures can be carried out for only a few substances.

Several methods for estimating low-temperature vapor pressures are found in the literature. The method described by Baehr [1] uses differences of the internal energy which are related to the first and second temperature derivatives of the vapor pressure. The thermal-loop calculations developed by Yarbrough and Tsai [2] and used by Goodwin [3] are also based on an integration of the Clausius–Clapeyron equation requiring the knowledge of the saturated liquid heat capacity C_σ. A similar method is used by Weber [4], who uses measured C_σ-values to check the consistency of low-temperature vapor pressure data. However, differences of internal energy or saturated liquid heat capacities are seldom measured, and therefore, these methods can be applied for a few fluids only.

In this paper, a new estimation method for vapor pressures at low temperatures is presented. It is based on a regression analysis of available experimental vapor pressures using the Clausius–Clapeyron equation and a simple relation for the enthalpy of vaporization. No experimental data on properties such as internal-energy differences or saturated liquid heat capacities are needed. Results are given for the triple-point pressures and the vapor pressure at low temperatures for R125, R32, R143a, R134a, R152a, R123, R124, and ammonia. A further result of this method is an equation for the enthalpy of vaporization at. low temperatures. This method is also useful to check the reliability of experimental vapor-pressure data or to determine inconsistencies between enthalpy of vaporization data and vapor pressures at low temperatures.

2. THEORETICAL MODEL

The general relationship among vapor pressure, saturated specific volumes, and specific enthalpy of vaporization Δh_v on which this model is based is given by the Clausius–Clapeyron relation, Eq. (1). It is transformed into

$$-\frac{d\ln p_s}{d\tau}=\frac{\Delta h_v(T)/(RT^*)}{Z''(T)-Z'(T)} \tag{2}$$

where $\tau = T^*/T$ is the inverse reduced temperature, T^* is an arbitrary reduction parameter, and $R = R_m/M$ is the individual gas constant with the molar mass M and $R_m = 8.314471\ \mathrm{J\cdot mol^{-1}\cdot K^{-1}}$ [5]. $Z'' = (p_s v'')/(RT)$ is the compressibility factor for saturated vapor and $Z' = (p_s v')/(RT)$ for saturated liquid.

Integration of Eq. (2) leads to

$$\ln \frac{p_s(T_0)}{p_s(T)} = \int_{\tau_0}^{\tau} \frac{\Delta h_v(T)/(RT^*)}{Z''(T) - Z'(T)} d\tau \tag{3}$$

where $p_s(T_0)$ is the vapor pressure for an arbitrary temperature T_0. Typically, the integral in Eq. (3) must be solved numerically due to the combination of three temperature functions. The numerical integration is carried out in this work by the area method. For a very small temperature change ΔT, the argument of the integral can be regarded as almost-constant, and Eq. (3) is approximated by

$$\ln \frac{p_s(T_0)}{p_s(T_0 + \Delta T)} \approx \frac{\Delta h_v(\bar{T})}{RT^*[Z''(\bar{T}) - Z'(\bar{T})]} \Delta\tau \tag{4}$$

The temperature functions Z'', Z', and Δh_v are evaluated at the temperature

$$\bar{T} = T_0 + \Delta T/2 \tag{5}$$

$\Delta\tau$ is the difference of inverse reduced temperatures corresponding to ΔT:

$$\Delta\tau = \frac{T^*}{T_0 + \Delta T} - \frac{T^*}{T_0} \tag{6}$$

The pressure ratio for any temperature interval can be calculated by dividing the interval into subsections of the size ΔT and multiplying the pressure ratios for all subsections. Other numerical integration methods cannot be applied because the vapor pressure in an interval ΔT is necessary to calculate Z'', leading to an iteration in each interval ΔT.

At low temperatures and vapor pressures, the compressibility factor Z'' of the saturated vapor can be calculated from a virial equation of state,

$$Z'' = \frac{p_s v''}{RT} = 1 + \frac{B(T)}{v''} = 1 + \frac{B(T)\, p_s}{RT} \tag{7}$$

truncated after the second virial coefficient. For most substances, Eq. (7) generally yields compressibility factors with an accuracy better than ± 0.01 for pressures up to 500 kPa. At temperatures well below the normal boiling point, even the influence of the second virial coefficient $B(T)$ might be neglected. Since the second virial coefficient is generally available, it is always taken into account in the following work.

A temperature function for the saturated liquid volume is also often available. However, the influence of Z' on $d(\ln p_s)/dT$ is very small since it is subtracted from Z'', which is about two to four orders of magnitude greater than Z'. This means that an error of 10% for the saturated liquid volume would affect the vapor pressure derivative by 0.1% or less. Further discussion of the influence of Z' is given in Section 3.

The third and most important temperature function required for the integration is an equation for the enthalpy of vaporization $\Delta h_v(T)$ For this work, this equation must be capable of accurately representing the enthalpy of vaporization for low temperatures and, more importantly, should allow safe extrapolation to even lower temperatures.

Several forms of a suitable $\Delta h_v(T)$ equation were discussed recently by Svoboda et al. [6]. For the present purposes, Svoboda et al. [6] recommend simple equations with two or three adjustable parameters. Such an equation is the relation proposed by Watson [7], which can be written as

$$\Delta h_v(T) = \Delta h_0(1 - T/T^*)^n \tag{8}$$

and which has been chosen for this work. In most cases the critical temperature T_c is used for T^*. A common choice for n is a value between 0.375 and 0.38, for which the temperature dependence of the enthalpy of vaporization is well described from the triple point to the critical point for many fluids (cf. Ref. 8). Svoboda found that, for temperatures below the normal boiling point, Eq. (8) can be accurate within $\pm 0.05\%$ with $n = 0.375$.

For a temperature range restricted to lower temperatures, it is assumed that the exponent n could have a value slightly different from 0.375 or 0.38 in order to give an optimal representation of the enthalpy of vaporization. Alternatively, another reducing temperature different from T_c might be used while n is kept constant. In both cases, there are two adjustable parameters in Eq. (8): $\{\Delta h_0, n\}$ or $\{\Delta h_0, T^*\}$. Since the relations for $Z''(T)$ and $Z'(T)$ are assumed to be known, these are the only unknowns in the entire extrapolation model.

The easiest way to determine these parameters for a certain fluid would be to fit Eq. (8) to experimental data of the enthalpy of vaporization. However, since this property has been measured for only a few fluids, this approach is seldom feasible. Experimental data which are available more readily are vapor pressures around the normal boiling point. Such data still lie within the range of validity of the extrapolation model. Thus, they can alternatively be used to determine the coefficients of Eq. (8).

Given initial values for $\{\Delta h_0, n\}$ or $\{\Delta h_0, T^*\}$, functions for $Z''(T)$ and $Z'(T)$, and an initial vapor pressure $p_s(T_0)$, the vapor pressure

$p_s^{calc}(T^{meas})$ can be calculated from Eq. (4) at the temperature T_i^{meas} for which an experimental vapor pressure $p_s^{meas}(T_i^{meas})$ exists. Calculated and measured vapor pressures are compared and the coefficients of the model are adjusted to improve the representation of a set of measured vapor pressures. This leads to a nonlinear optimization process where the sum of squares,

$$S = \sum_{i=1}^{M} [p_s^{meas}(T_i^{meas}) - p_s^{calc}(T_i^{meas})]^2 \sigma_{p,i}^{-2} \tag{9}$$

has to be minimized. $\sigma_{p,i}$ is the total standard deviation of an experimental vapor pressure estimated from experimental uncertainties according to the Gaussian error propagation law. The nonlinear regression strategy developed by Dennis et al. [9] has been used to optimize the parameters.

It was decided to include the initial pressure $p_s(T_0)$ as an adjustable parameter. Using a fixed value for $p_s(T_0)$ would cause any inaccuracy of its value to propagate to extrapolated vapor pressures. Since the choice of the temperature T_0 is arbitrary, the triple-point pressure $p_s(T_{tr}) = p_{tr}$ was chosen for $p_s(T_0)$. The two possible sets of parameters, $\{\Delta h_0, n, p_{tr}\}$ or $\{\Delta h_0, T^*, p_{tr}\}$, to be optimized are examined in Section 4.

3. ANALYSIS OF ERROR PROPAGATION

Before carrying out vapor-pressure extrapolations, the propagation of possible errors in Z', Z'', and Δh_v is investigated. The contribution of one of these properties to a vapor pressure calculated from Eq. (4) is conveniently illustrated by analyzing the argument of the integral,

$$\arg(T) = \frac{\Delta h_v(T)/(RT^*)}{Z''(T) - Z'(T)} \tag{10}$$

This is plotted versus the inverse reduced temperature τ in Fig. 1. The area under $\arg(T)$ between two temperatures T_0 and T_1 is identical to the logarithm of the pressure ratio, $\ln[p_s(T_1)/p_s(T_0)]$. Any change of the models for Z', Z'', or Δh_v will produce a change of area and thus a change in the vapor-pressure ratio. When using a preset value for $p_s(T_1)$, the vapor pressure $p_s(T_0)$ at the low-temperature limit can be calculated and any variation of Z', Z'', or Δh_v is transformed into a variation of $p_s(T_0)$. This variation is taken as a measure for the propagation of errors previously applied to $Z'(T)$, $Z''(T)$, or $\Delta h_v(T)$.

In the example shown in Fig. 1, the "true" shape of $\arg(T)$ was obtained with Z', Z'', and Δh_v calculated from the fundamental equation of state for R134a established by Tillner-Roth and Baehr [10]. The

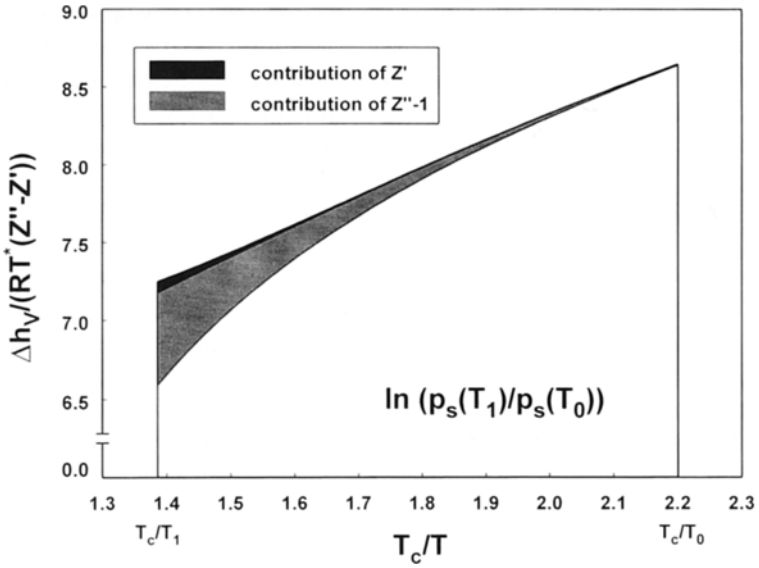

Fig. 1. Contributions of Z'' and Z' to the integral of the Clausius–Clapeyron equation, Eq. (3), applied to R134a for $T_0 = 170$ K and $T_1 = 270$ K. The curves were calculated using thermodynamic properties generated from the fundamental EOS by Tillner-Roth and Baehr [10].

integration boundaries were chosen as $T_0 = 170$ K and $T_1 = 270$ K. From the resulting pressure ratio the vapor pressure $p_s(T_0)$ was calculated with $p_s(T_1) = 260824.21$ Pa obtained from the equation of state. The results for different variations of Z', Z'', and Δh_v are summarized in Table I.

The greatest deviation from the reference pressure value occurs when the real behavior in the vapor phase is neglected by setting $Z'' = 1$. The error of about 12% for $p_s(T_0)$ is due mainly to the large real gas contribution at high temperatures. This is illustrated by the gray area in Fig. 1 which becomes large when approaching T_c/T_1. This large error of $p_s(T_0)$ is almost eliminated when taking into account only the second virial coefficient. For lower temperatures (increasing values of T_c/T), the influence of real-gas behavior becomes progressively smaller. Therefore, an error in the second virial coefficient at low temperatures would have only a minor influence on the extrapolated vapor pressure. The influence of the saturated-liquid compressibility factor Z' is almost negligible as indicated by the black area in Fig. 1. When setting $Z' = 0$, the error of the extrapolated vapor pressure does not exceed 1%. When v' is set to a constant nonzero value, as to the saturated liquid volume at the normal boiling point, the error in $p_s(T_0)$ drops below 0.01%.

Table I. Influence of Z'', Z', and Δh_v on the Vapor Pressure Calculated from Eq. (4)[a,b]

Δh_v	Z''	Z'	$\ln\frac{p_s(T_1)}{p_s(T_0)}$	$\frac{p_s(T_1)}{p_s(T_0)}$	$\frac{p_s(T_0)}{\text{(Pa)}}$	$100\frac{\varepsilon_{p_s}}{p_s}$
Δh_v	$Z''(T)$	$Z'(T)$	6.48976	658.365	396.170	—
Δh_v	1	$Z'(T)$	6.37180	585.112	445.768	+12.52
Δh_v	$1+(B/v'')$	$Z'(T)$	6.48914	657.957	396.415	+0.06
Δh_v	$Z''(T)$	0	6.47985	651.873	400.115	+1.00
Δh_v	$Z''(T)$	$(p_s v')_{NB}/(RT)$	6.48973	658.345	396.181	<0.01
$1.005\cdot\Delta h_v$	$Z''(T)$	$Z'(T)$	6.50273	666.960	391.064	−1.29
Δh_v	$1+1.05\cdot(B/v'')$	$Z'(T)$	6.49528	662.010	393.988	−0.55
Δh_v	$Z''(T)$	$1.01\cdot Z'(T)$	6.48985	658.425	396.133	−0.01

[a] $T_0 = 170$ K, $T_1 = 270$ K, $\varepsilon_{p_s} = p_s(T_0) - p_s^{EOS}(T_0)$; NB, normal boiling point.
[b] All thermodynamic properties are calculated from the fundamental EOS for R134a by Tillner-Roth and Baehr [10].

The last three calculations in Table I show the effect of systematic offsets applied to Δh_v, B, and Z'. The greatest effect is observed for a change of the enthalpy of vaporization of +0.5% in the whole temperature range, leading to a deviation of the extrapolated pressure of about 1.3%. A change of the second virial coefficient affects the vapor pressure to a smaller extent. A 5% change of B gives a 0.55% change in pressure, because B contributes significantly to the pressure ratio only at high temperatures. A 1% change of v' or Z' has almost no effect on the extrapolated pressure.

These calculations show that it is important to take into account the second virial coefficient to calculate Z'' when the integration starts at temperatures around the normal boiling point. Systematic errors in B affect the extrapolation primarily at higher temperatures. For decreasing temperatures, the real-gas contribution loses influence, and even relatively large errors in B would have no-significant influence on the vapor-pressure extrapolation. The influence of the saturated-liquid volume is small. Inaccuracies of the enthalpy of vaporization have the largest effect on an extrapolated pressure. The coefficients of Eq. (8) should be as reliable as possible to ensure an accurate integration of the Clausius–Clapeyron equation.

4. RESULTS

The extrapolation procedure has been applied to generate low-temperature vapor pressures for R125 (pentafluoroethane), R32 (difluoromethane),

R143a (1,1,1-trifluoroethane), R134a (1,1,1,2-tetrafluoroethane), R152a (1,1-difluoroethane), R124 (1-chloro-1,2,2,2-tetrafluoroethane), and R123 (1,1-dichloro-2,2,2-trifluoroethane). Ammonia (NH_3) has also been chosen because there are experimental enthalpies of vaporization available for comparisons of the resulting Δh_v equation.

The second virial coefficient has been calculated from the generalized model established by Weber [11] for the seven refrigerants. For ammonia, B has been calculated from the fundamental equation of state established by Tillner-Roth et al. [12].

Saturated liquid densities at the normal boiling point were obtained for R134a, R152a, R123, and ammonia from Ref. 13. For R125, R32, R143a, and R124, they were obtained from the REFPROP database program [14]. The tables in Ref. 13 as well as REFPROP calculations are based on multiparametric equations of state of high accuracy. An overview of the fluid properties important for this work is given in Table II along with the sources of experimental vapor pressures used to optimize the adjustable parameters. The properties for R134a, R152a, R123, and ammonia were obtained from Ref. 13, those for R143a, R125, R32, and R124 from Ref. 14.

Table II. Characteristic Constants and Vapor-Pressure Data of Investigated Refrigerants

Fluid	M ($g \cdot mol^{-1}$)[a]	T_c (K)[b]	T_{NB} (K)[c]	ϱ'_{NB} ($kg \cdot m^{-3}$)[d]	Ref. No.[e]	N_v all/used[f]	T range (K)[g]	p range (kPa)[g]
R125	120.02	339.33	225.007	1515.0	19	104/87	218–269	73–601
					20	33/20	215–270	60–605
R32	54.024	351.35	221.493	1212.8	22	27/27	208–237	49–214
					19	17/13	235–259	200–500
R143a	84.041	346.04	224.739	1167.6	15	31/31	236–280	160–751
R134a	102.032	374.18	247.076	1376.7	27	57/51	214–289	17–504
R152a	66.051	386.41	249.132	1010.8	16	36/31	200–260	6–160
					29	43/22	207–263	10–179
R124	136.475	395.425	261.140	1473.6	19	39/39	221–286	14–259
					34	70/18	278–298	195–382
R123	152.931	456.831	300.967	1456.7	36	61/43	256–335	14–299
NH_3	17.03026	405.34	239.824	682.0	32	150/118	224–303	45–1166
					18	11/4	224–241	44–111

[a] Molar mass.
[b] Critical temperature.
[c] Temperature at normal boiling point.
[d] Saturated-liquid density at normal boiling point.
[e] Reference No. of experimental data.
[f] Number of experimental vapor pressures.
[g] Ranges refer only to experimental data used in this work.

4.1. Triple-Point Pressures

In every optimization process, the results for the adjusted parameters depend on the experimental data selected for the fit. Other than the accuracy of the data, the range of data also influences the optimization result. To determine the optimal parameter values, the length of the data interval must be varied and a set of regressions must be performed.

A set of vapor pressure data can be characterized by its lower and upper temperature limits T_{min} and T_{max}. If T_{max} is too high, the extrapolation might become worse because effects of the third virial coefficients are not taken into account or the simple Δh_v equation might not be sufficient to describe a large temperature interval properly. On the other hand, a data interval might be too short to ensure a reliable fit of the coefficients. Therefore, it is necessary to determine the data interval for which the most reliable results for the adjustable parameters are obtained.

Table III. Triple-Point Temperatures T_{tr} and Triple-Point Pressures p_{tr}

Fluid	T_{tr} (K)	ΔT_p (K)[a]	Adjusted parameters	$\bar{p}_{tr}$ (Pa)[b]	p_{tr} (Pa) Calc.	p_{tr} (Pa) Meas.
R125	172.52 [31]	235–250	$(\Delta h_0, n, p_{tr})$	2961.0 ± 8.0	2921 [14]	n.a.
			$(\Delta h_0, T^*, p_{tr})$	2955.0 ± 7.0		
R32	136.34 [31]	230–250	$(\Delta h_0, n, p_{tr})$	51.26 ± 0.17	48 [14]	n.a.
			$(\Delta h_0, T^*, p_{tr})$	50.70 ± 0.14		
R143a	161.34 [31]	240–253	$(\Delta h_0, n, p_{tr})$	1080.0 ± 25.0	1061 [14]	n.a.
			$(\Delta h_0, T^*, p_{tr})$	1091.0 ± 6.0		
R134a	169.85 [39]	231–265	$(\Delta h_0, n, p_{tr})$	402.3 ± 2.3	389.6 [10]	n.a.
			$(\Delta h_0, T^*, p_{tr})$	402.3 ± 1.4	392.4 [14]	
R152a	154.56 [16]	230–248	$(\Delta h_0, n, p_{tr})$	65.87 ± 0.28	65.4 [30]	65 [16]
			$(\Delta h_0, T^*, p_{tr})$	65.85 ± 0.25	64.07 [14]	
R124	150.00[c]	258–273	$(\Delta h_0, n, p_{tr})$	12.10 ± 0.10	11.07 [14]	n.a.
			$(\Delta h_0, T^*, p_{tr})$	12.10 ± 0.08		
R123	166.00[d] [37]	270–295	$(\Delta h_0, n, p_{tr})$	4.73 ± 0.05	4.20 [37]	n.a.
			$(\Delta h_0, T^*, p_{tr})$	4.74 ± 0.04		
NH_3	195.495 [17]	260–300	$(\Delta h_0, n, p_{tr})$	6072.0 ± 7.0	6091 [12]	6026 [17]
			$(\Delta h_0, T^*, p_{tr})$	6063.0 ± 6.0	6077 [38]	6077 [18]

[a] Range of plateaus (cf. Fig. 2).

[b] Averaged from the results of nonlinear regressions.

[c] According to Magee [31], R124 transforms into a glass around 75 K. The value of 150 K was chosen arbitrarily.

[d] R123 transforms also into a glass around 166 K and has no defined triple point. The value of 166 K was chosen by Younglove and McLinden [37] as the triple-point temperature for their equation of state and was, therefore, also used for this work.

For the regressions, the lower temperature limit T_{min} of the data interval was kept constant. It corresponds to the lowest limit of the temperature ranges given in Table II for each fluid. Therefore, the data interval can be characterized by the upper temperature limit T_{max} only. T_{max} was varied in steps of 1 K starting from the upper temperature limit of the selected data down to a temperature where at least five data points remain in the data interval. During each regression vapor pressures are calculated between the chosen value of T_{max} and the respective triple-point temperature listed in Table III. Two types of regressions were performed adjusting either $\{\Delta h_0, n, p_{tr}\}$ or $\{\Delta h_0, T^*, p_{tr}\}$. In the first case, the critical temperature T_c

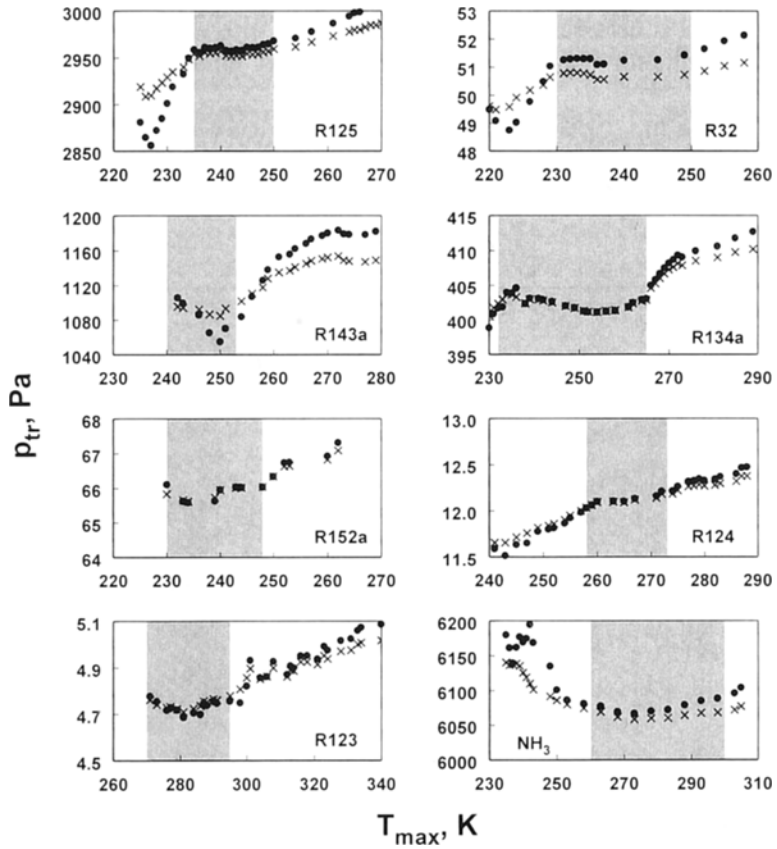

Fig. 2. Triple-point pressures estimated from nonlinear regressions. T_{max}, upper temperature limit of the input data; ●, results for the optimization of $\{\Delta h_0, n, p_{tr}\}$; ×, results for the optimization of $\{\Delta h_0, T^*, p_{tr}\}$. The shaded areas indicate the plateau ranges.

was chosen for T^*. In the second case, a constant value of O.375 was used for the exponent n. The optimization results for the triple-point pressures are plotted over T_{max} in Fig. 2 for both types of regression.

In most cases the estimated triple-point pressure decreases for decreasing values of T_{max} until the values form a plateau over a certain range of T_{max}. Here, the optimized triple-point pressure is almost independent of the range of experimental data. When T_{max} is further decreased, that is, when the number of input data becomes smaller, the scatter of data becomes larger or a further drop or rise in the estimated triple-point pressure occurs. This behavior is the same for both types of regressions. However, the variation of p_{tr} is smaller when $\{\Delta h_0, T^*, p_{tr}\}$ is optimized. These regressions produce more stable results and therefore, are regarded to be of higher reliability.

The most reliable estimates for the parameters are presumably obtained when p_{tr} is independent of the chosen data set. The optimized triple-point pressures are arithmetically averaged from the regressions located within the plateau range. These average values are given in Table III for both types of regressions for all fluids. The uncertainties listed in Table III correspond to the maximum deviation from the arithmetic mean.

Generally, the uncertainty is smaller for the regressions using $\{\Delta h_0, T^*, p_{tr}\}$, so the reliability is higher. The triple-point pressures from these regressions are usually slightly lower than from the other type of regression. This is due to the constant exponent $n = 0.375$, which is sometimes slightly higher than the n values from the $\{\Delta h_0, n, p_{tr}\}$ regressions. This causes a stronger temperature dependence of Δh_v and, thus, a larger pressure ratio.

For all fluids except R143a, the plateau ranges are clearly defined. In the case of R143a two possible plateau ranges are observed. The first range occurs at T_{max} values above 270 K, yielding a triple-point pressure around 1140 Pa. The second plateau range is observed only for the regressions fitting $\{\Delta h_0, T^*, p_{tr}\}$ when T_{max} is between 242 and 252 K. The resulting triple-point pressure of around 1090 is about 50 Pa lower. The reason for the occurrence of two plateaus is a structural break in the vapor-pressure measurements by Weber [15], which can be seen more clearly in Fig. 3. Regressions with low T_{max} values are based on the pressures at low temperatures only, while regressions with T_{max} values higher than 245 K include also the data at higher temperatures having a different characteristic. Thus, the different triple-point pressures determined for the two plateaus reflect the inconsistency of Weber's measurements. The regression analysis is obviously extremely sensitive to inaccuracies of the experimental input data even when they are of the order of only 0.1 % or less, as for R143a. This makes this method also a useful tool for checking experimental data.

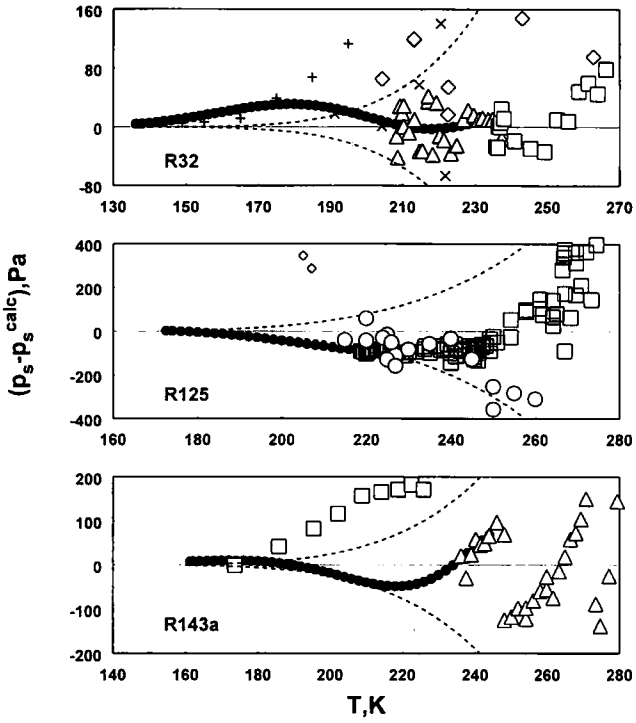

Fig. 3. Vapor-pressure comparisons. (●) This work. R32: ×; Malbrunot et al. [23]; +, Kanungo et al. [24]; △, Weber and Goodwin [22]; □, Weber and Silva [19]; ◇, Türk et al. [29]. R125: □, Weber and Silva [19]; ◇, Türk et al. [29]; ○, Magee [20]. R143a: △, Weber [15]; □, Russell et al. [25]; baseline; vapor-pressure equations by Outcalt and McLinden [21] (R32, R125) and by Outcalt [26] (R143a); – – – –, ±0.1%.

The better estimate for the triple-point pressure is probably obtained from the plateau at lower T_{max} values, because the pressure of data points above 270 K reaches 0.8 MPa, which is well above the limit where the extrapolation model can be safely applied. It would be desirable to conduct regressions at T_{max} values below 242 K, but currently no reliable vapor-pressure data are available at temperatures below 236 K.

The optimized triple-point pressures are compared with results from other sources in Table III. Excellent agreement is observed for R152a with the value of 65 Pa measured by Blanke and Weiss [16]. The estimated triple-point pressure of ammonia lies between the measurement of McKelvy and Taylor [17] and that of Overstreet and Giauque [18]. Agreement is within 37 Pa, or 0.6%. For the other fluids, no experimental

triple-point pressures are available, but values were calculated from various equations of state using the respective triple-point temperatures from Table III. The extrapolated triple-point pressures agree with calculated values within a few pascals. For some of the fluids for which no experimental triple-point pressure is available, comparisons with experimental vapor pressures above the triple point are given in the next section.

All further investigations are based on the triple-point pressure obtained from the $\{\Delta h_0, T^*, p_{tr}\}$ regressions. No more work was carried out on the $\{\Delta h_0, n, p_{tr}\}$ regressions.

4.2. Vapor Pressure and Enthalpy of Vaporization

With any set of parameters $\{\Delta h_0, T^*, p_{tr}\}$, the vapor pressure can be calculated for any desired temperature. However, the triple-point pressures were averaged in Section 4.1. Therefore, Δh_0 and T^* were readjusted using the previously determined averages for p_{tr} as fixed values. Only those regressions were repeated which are based on data intervals with T_{max} lying in the plateau ranges (Fig. 2). The resulting coefficients, Δh_0 and T^*, were arithmetically averaged and are given for the different fluids in Table IV. The uncertainties correspond again to the maximum scatter of the regression results. With these values, vapor pressures were calculated from the triple-point up to a temperature equal to the lowest value of T_{max} used during this last regression analysis. The vapor pressures are listed in Table V in steps of 2 K. The maximum uncertainty given for each fluid in Table V corresponds to the maximum variation of vapor pressures estimated during all single regressions. These uncertainties also take into account the results from the regression analysis during which the triple-point pressure

Table IV. Coefficients for the Δh_v Equation, Eq. (8),[a] Averaged from Nonlinear Regressions

Fluid	Δh_0 ($kJ \cdot kg^{-1}$)	T^* (K)
R125	244.551 ± 0.042	344.784 ± 0.040
R32	544.820 ± 0.080	362.098 ± 0.040
R143a	332.872 ± 0.884	351.992 ± 0.631
R134a	325.352 ± 0.226	374.933 ± 0.183
R152a	485.465 ± 0.363	386.278 ± 0.215
R124	249.220 ± 0.096	396.471 ± 0.112
R123	256.778 ± 0.070	453.643 ± 0.093
NH_3	1885.870 ± 1.207	419.108 ± 0.189

[a] $n = 0.375$.

Table V. Extrapolated Vapor Pressures

T (K)	p_s (Pa)	T (K)	p_s (Pa)	T (K)	p_s (Pa)	T (K)	p_s (Pa)	T (K)	p_s (Pa)
				R125 ($\varepsilon_{max} = \pm 9.5$ Pa)[a]					
172.52	2,955.0	184	7,848.5	196	18,899.4	208	40,429.7	220	78,504.4
174	3,380.2	186	9,171.4	198	21,616.2	210	45,439.4	222	86,972.1
176	4,036.6	188	10,675.7	200	24,645.4	212	50,937.5	224	96,146.8
178	4,798.1	190	12,380.0	202	28,013.3	214	56,957.8	226	106,068.8
180	5,677.6	192	14,304.4	204	31,747.2	216	63,534.9	228	116,779.3
182	6,689.4	194	16,470.1	206	35,876.0	218	70,704.8	230	128,320.3
				R32 ($\varepsilon_{max} = \pm 6.6$ Pa)					
136.34	50.7	156	682.3	176	4,947.9	196	22,751.0	216	75,984.7
138	65.2	158	853.5	178	5,866.8	198	25,992.9	218	84,544.0
140	87.5	160	1,061.0	180	6,926.3	200	29,606.2	220	93,859.9
142	116.4	162	1,310.9	182	8,143.0	202	33,622.2	222	103,979.1
144	153.5	164	1,610.1	184	9,535.0	204	38,074.0	224	114,950.3
146	200.6	166	1,966.6	186	11,121.5	206	42,996.2	226	126,823.2
148	260.1	168	2,389.1	188	12,923.3	208	48,425.0	228	139,649.0
150	334.6	170	2,887.2	190	14,962.7	210	54,398.1	230	153,480.4
152	427.3	172	3,471.6	192	17,263.4	212	60,954.9	232	168,371.2
154	541.8	174	4,154.2	194	19,850.6	214	68,136.3		
				R143a ($\varepsilon_{max} = \pm 49.2$ Pa)					
161.34	1,091.0	178	5,056.7	196	19,009.7	214	55,454.0	232	133,973.0
162	1,167.4	180	5,947.7	198	21,650.5	216	61,676.4	234	146,368.6
164	1,427.6	182	6,967.0	200	24,584.3	218	68,443.7	236	159,638.8
166	1,736.2	184	8,128.7	202	27,834.8	220	75,789.2	238	173,823.9
168	2,100.3	186	9,448.0	204	31,426.9	222	83,746.8	240	188,965.1
170	2,527.8	188	10,941.0	206	35,386.4	224	92,351.6	242	205,103.8
172	3,027.2	190	12,624.9	208	39,740.3	226	101,639.5	244	222,282.2
174	3,608.2	192	14,517.9	210	44,516.6	228	111,647.2		
176	4,280.9	194	16,639.3	212	49,744.5	230	122,412.3		
				R134a ($\varepsilon_{max} = \pm 4.5$ Pa)					
169.85	402.3	182	1,389.5	196	4,655.5	210	12,934.5	224	30,948.5
170	409.0	184	1,673.4	198	5,443.9	212	14,774.7	226	34,693.1
172	508.4	186	2,006.0	200	6,342.4	214	16,827.2	228	38,798.4
174	628.3	188	2,393.9	202	7,363.0	216	19,110.3	230	43,289.7
176	772.3	190	2,844.5	204	8,518.4	218	21,643.2	232	48,192.9
178	944.1	192	3,365.6	206	9,822.3	220	24,446.3		
180	1,148.2	194	3,966.2	208	11,289.1	222	27,540.6		

[a] Maximum variation of vapor pressure of all single regressions.

Table V. *(Continued)*

T (K)	p_s (Pa)	T (K)	p_s (Pa)	T (K)	p_s (Pa)	T (K)	p_s (Pa)	T (K)	p_s (Pa)
				R152a ($\varepsilon_{max} = \pm 5.6$ Pa)					
154.56	65.85	170	418.5	186	1,974.9	202	7,042.6	218	20,260.2
156	79.63	172	517.3	188	2,347.2	204	8,123.0	220	22,832.1
158	103.0	174	636.0	190	2,778.0	206	9,338.8	222	25,665.7
160	132.3	176	777.8	192	3,274.5	208	10,703.0	224	28,780.5
162	168.7	178	946.2	194	3,844.7	210	12,229.5	226	32,196.9
164	213.7	180	1,145.4	196	4,497.0	212	13,932.7	228	35,935.9
166	269.0	182	1,379.8	198	5,240.7	214	15,828.0	230	40,019.6
168	336.5	184	1,654.5	200	6,085.7	216	17,931.5	232	44,470.7
				R124 ($\varepsilon_{max} = \pm 14.6$ Pa)					
150	12.10	174	266.5	198	2,533.7	222	13,788.8	246	51,102.9
152	16.33	176	330.4	200	2,972.1	224	15,577.5	248	56,233.2
154	21.85	178	407.3	202	3,473.3	226	17,553.2	250	61,766.2
156	28.99	180	499.5	204	4,044.6	228	19,730.4	252	67,723.9
158	38.16	182	609.4	206	4,693.6	230	22,124.4	254	74,128.7
160	49.84	184	739.8	208	5,428.4	232	24,750.7	256	81,003.5
162	64.61	186	893.8	210	6,257.8	234	27,625.9	258	88,371.9
164	83.2	188	1,074.8	212	7,191.2	236	30,767.0	260	96,257.7
166	106.4	190	1,286.7	214	8,238.6	238	34,191.7		
168	135.1	192	1,533.6	216	9,410.5	240	37,918.4		
170	170.4	194	1,820.3	218	10,718.1	242	41,966.0		
172	213.8	196	2,151.9	220	12,173.4	244	46,354.1		
				R123 ($\varepsilon_{max} = \pm 3.5$ Pa)					
166	4.74	188	75.5	210	629.6	232	3,324.7	254	12,579.3
168	6.30	190	93.7	212	744.7	234	3,798.5	256	14,008.4
170	8.32	192	115.7	214	877.7	236	4,328.4	258	15,568.9
172	10.91	194	142.1	216	1,030.8	238	4,919.5	260	17,269.9
174	14.20	196	173.8	218	1,206.5	240	5,577.3	262	19,120.6
176	18.36	198	211.6	220	1,407.5	242	6,307.5	264	21,130.7
178	23.58	200	256.4	222	1,636.6	244	7,116.4	266	23,310.4
180	30.11	202	309.4	224	1,897.1	246	8,010.3	268	25,670.0
182	38.21	204	371.8	226	2,192.3	248	8,996.3	270	28,220.4
184	48.20	206	444.9	228	2,525.9	250	10,081.3	272	30,972.6
186	60.47	208	530.2	230	2,902.0	252	11,273.0		
				Ammonia ($\varepsilon_{max} = \pm 48.7$ Pa)					
195.495	6,063.0	208	15,432.2	222	38,115.1	236	83,333.9	250	164,968.5
196	6,312.8	210	17,709.6	224	42,915.6	238	92,391.6	252	180,599.5
198	7,390.4	212	20,262.7	226	48,204.7	240	102,233.0	254	197,392.3
200	8,620.9	214	23,117.1	228	54,019.3	242	112,907.0	256	215,407.1
202	10,021.3	216	26,300.0	230	60,398.2	244	124,464.3	258	234,706.3
204	11,609.9	218	29,840.2	232	67,381.9	246	136,957.4	260	255,353.2
206	13,406.5	220	33,767.9	234	75,012.5	248	150,440.2	262	277,413.0

was also fitted. The data from Table V are compared with experimental vapor pressures in Figs. 3 to 5. Different equations were used as baselines. References are given in the figure captions.

The regressions for R125 (Fig. 3) are based on the values measured by Weber and Silva [19] and by Magee [20]. Results from this study agree with the selected experimental data within 0.1%. No reliable measured values are available for temperatures below 210 K, but the extrapolated values agree very well with the vapor pressure equation of Outcalt and McLinden [21] used for the baseline.

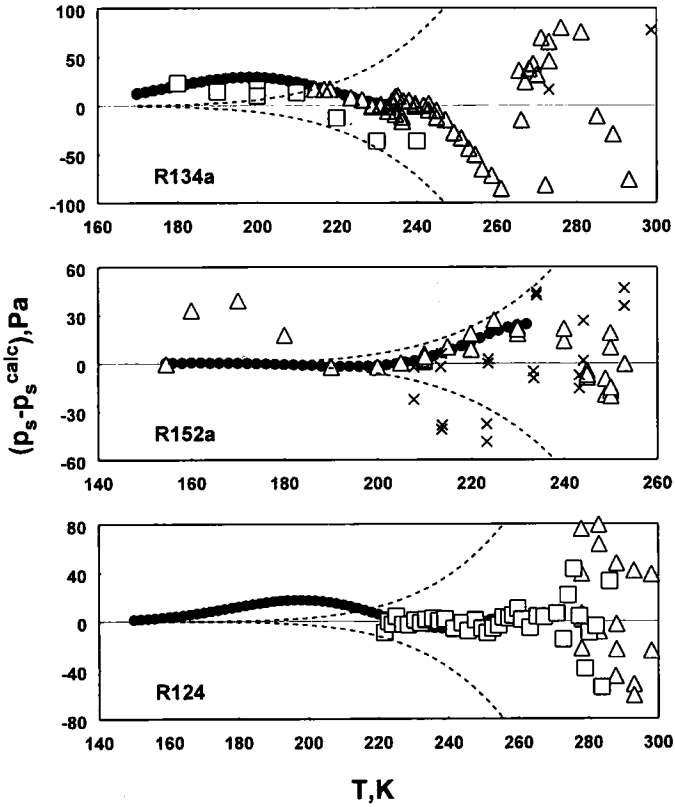

Fig. 4. Vapor-pressure comparisons. (●) This work. R134a: □, Magee and Howley [28]; △, Goodwin et al. [27]; ×, Türk et al. [29]; baseline, fundamental EOS by Tillner-Roth and Baehr [10]. R152a: △, Blanke and Weiss [16]; ×, Türk et al. [29]; baseline, fundamental EOS by Tillner-Roth [30]. R124: □, Weber and Silva [19]; △, Boyes and Weber [34]; baseline, vapor-pressure equation by Younglove [35]; ----, ±0.1%.

For R32 (Fig. 3), values of Weber and Goodwin [22] and of Weber and Silva [19] were used to fit the parameters. The data extend to 208 K. There are some data at lower temperatures measured by Malbrunot et al. [23] and some calculated values by Kanungo et al. [24]. They show systematic deviations from the zero line but agree with extrapolated vapor pressures for temperatures below 190 K within ± 10 Pa.

For R143a (Fig. 3), the structural break in the results of Weber [15], mentioned in Section 4.1, is clearly observed although this break is less than 0.1%. The results reported by Russell et al. [25] show positive systematic deviations from the present values at high temperatures, but both series converge at lower temperatures. The extrapolated values are almost identical with the values calculated from the vapor-pressure equation of Outcalt [26] at temperatures below 190 K.

The results for R134a (Fig. 4) are based only on the data of Goodwin et al. [27]. The extrapolated values below 214 K show excellent agreement with the results of Magee and Howley [28]. However, they show a positive systematic deviation of about 30 Pa from the baseline, which is the fundamental equation of state established by Tillner-Roth and Baehr [10]. The good agreement between extrapolated and measured values and the systematic deviation from the baseline could indicate a small systematic error of the equation of state.

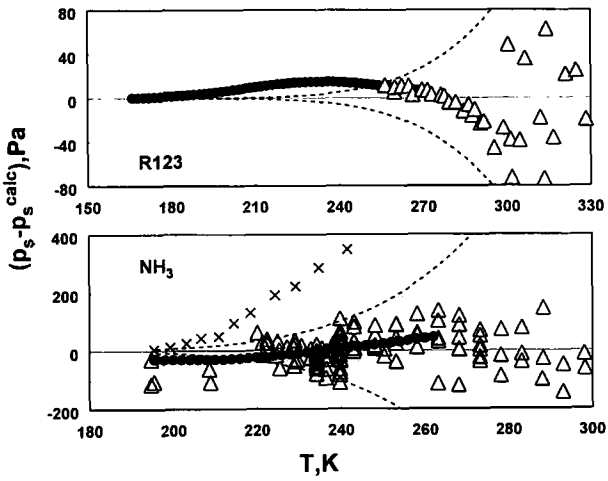

Fig. 5. Vapor-pressure comparisons. (●) This work. R123: △, Goodwin et al. [36]; baseline, fundamental EOS by Younglove and McLinden [37]. NH_3: △, Cragoe et al. [32]; ×, Overstreet and Giauque [18]; baseline, fundamental EOS by Tillner-Roth et al. [12]; – – – –, ± 0.1%.

The most satisfying result was obtained for R152a (Fig. 4.) Here, the extrapolation was based on the results of Blanke and Weiss [16] above 200 K and on those of Türk et al. [29]. The extrapolated values below 200 K agree within 1 or 2 Pa with the fundamental equation of state established by Tillner–Roth [30] used as a baseline. The extrapolated values also reveal systematic differences for the vapor pressures of Blanke and Weiss [16] at 160, 170, and 180 K.

For R124 (Fig. 4) and for R123 (Fig. 5), no data are available for temperatures below those of the measured vapor pressures used for the regressions. However, the extrapolated values agree within 20 Pa with the equations used as baselines. No triple-point temperature is available for either substance. Magee [31] observed that R124 and R123 form glasses at low temperatures.

Figure 5 also shows the results for ammonia. The systematic difference between the data set of Cragoe et al. [32] and that of Overstreet and Giauque [18] is evident. The extrapolated values are generally located between both sets of measurements, but the present results suggest that the values of Cragoe et al. [32] at temperatures below 220 K could be slightly too low. The extrapolated values are also slightly lower than the fundamental equation of state established by Tillner-Roth et al. [12] used for the baseline.

Enthalpy of vaporization data are also available for ammonia. The data measured by Osborne and Van Dusen [33] are compared in Fig. 6 with Eq. (8) and the respective coefficients from Table IV. For temperatures below 270 K, Eq. (8) represents the experimental values within $\pm 0.5\%$. For higher temperatures the deviations become larger, possibly because Eq. (8) is not able to represent accurately the enthalpy of vaporization over wide ranges of temperatures or, alternatively, because of an

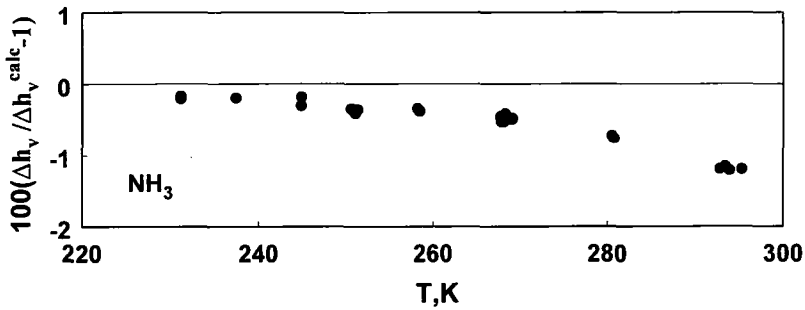

Fig. 6. Deviations of enthalpies of vaporization of ammonia from Eq. (8) using the coefficients from Table IV. ●, Osborne and Van Dusen [33].

inconsistency between the selected vapor pressures and enthalpies of vaporization. This is indicated by the small deviation of about 0.2 to 0.4% at low temperatures. Since the error is smaller for low temperatures, Eq. (8) is still suitable for an accurate extrapolation of the vapor pressure to lower temperatures, but use of the Δh_v-equation should be avoided at higher temperatures.

5. CONCLUSION

A thermodynamically consistent method to extrapolate vapor-pressure data to low temperatures for pressures less than approximately 0.1 MPa has been presented. This method involves a nonlinear regression analysis of a model based on the Clausius–Clapeyron relation and a simple equation for the enthalpy of vaporization. Only experimental vapor pressures at higher temperatures are needed as input data. This method has been employed to calculate vapor pressures and triple-point pressures for eight substances. The results were compared to experimental data and values calculated from various equations of state. The extrapolated pressures show good agreement with experimental data, in most cases within the experimental uncertainties. Thus, they can be used in developing comprehensive, multiparametric equations of state. The resulting equations for the enthalpy of vaporization are accurate within $\pm 0.5\%$ at low temperatures when accurate vapor pressures are used as input data. Further improvement of this model could be achieved by using more sophisticated equations for the enthalpy of vaporization or taking into account effects of higher-order virial coefficients. In doing so, vapor pressures even at higher temperatures could be used to establish the extrapolation model.

Apart from its extrapolation capability, this model is useful to detect inconsistencies within sets of vapor-pressure measurements. When enthalpy of vaporization data are available, the results of the regression analysis can also be used to check the consistency between enthalpy of vaporization data and vapor pressures. Finally, it should be mentioned that the extrapolated data are only as reliable as the experimental input data. Systematic errors in the latter reflect in the parameters of the extrapolation model and propagate also into the extrapolated vapor pressures.

ACKNOWLEDGMENTS

The author would like to thank J. W. Magee, L. A. Weber, B. A. Younglove, and S. Outcalt for supplying their results prior to publication and M. O. McLinden for his helpful advice. This work was carried out in part at the Thermophysics Division, NIST, Boulder.

REFERENCES

1. H. D. Baehr, *Forsch. Ing.-Wesen* **32**:1 (1966).
2. D. W. Yarbrough and C. H. Tsai, *Adv. Cryogen. Eng.* **23**:602 (1978).
3. R. D. Goodwin, *Isobutane: Provisional Thermodynamic Functions from 114 to 700 K at Pressures to 700 bar*, NBS Interagency Report No. 79-1612 (National Bureau of Standards, 1979).
4. L. A. Weber, *Int. J. Refrig.* **17**:117 (1994).
5. M. R. Moldover, J. P. M. Trusler, T. J. Edwards, J. B. Mehl, and R. S. Davis, *J. Res. Natl. Bur. Stand.* **93**:85 (1988).
6. V. Svoboda and P. Basarova, *Fluid Phase Equil.* **93**:167 (1994).
7. K. M. Watson, *Ind. Eng. Chem.* **35**:398 (1943).
8. R. C. Reid, J. M. Prausnitz, and B. E. Poling, *The Properties of Gases and Liquids*, 4th ed. (McGraw–Hill, New York, 1987).
9. J. E. Dennis, M. Gay, and R. E. Welsch, *An Adaptive Nonlinear Least-Squares Algorithm*, Technical Summary Report No. 2010 (Math. Res. Center, Madison, WI, 1979).
10. R. Tillner–Roth and H. D. Baehr, *J. Phys. Chem. Ref. Data* **23**:657 (1994).
11. L. A. Weber, *Int. J. Thermophys.* **15**:461 (1994).
12. R. Tillner–Roth, F. Harms-Watzenberg, and H. D. Baehr, *20th DKV-Tagung* (Heidelberg, Germany, 1993) Vol. II, p. 167.
13. H. D. Baehr and R. Tillner-Roth, *Thermodynamische Eigenschaften umweltverträlicher Kältemittel/Thermodynamic Properties of Environmentally Acceptable Refrigerants* (Springer-Verlag, Berlin, 1995).
14. J. S. Gallagher, M. L. Huber, G. Morrison, and M. O. McLinden, *NIST Standard Reference Database 23 (REFPROP), Version 4.0* (Stand. Ref. Data Program, NIST, Gaithersburg, MD, 1993).
15. L. A. Weber, personal communication (NIST, Thermophysics Division, Gaithersburg, MD), 1995.
16. W. Blanke and R. Weiss, *Fluid Phase Equil.* **80**:179 (1992).
17. E. C. McKelvey and C. S. Taylor, *Sci. Pap. Bur. Stands.* **18**:655 (1923).
18. R. Overstreet and W. F. Giauque, *J. Am. Chem. Soc.* **59**:254 (1937).
19. L. A. Weber and A. M. Silva, *J. Chem. Eng. Data* **39**:808 (1994).
20. J. W. Magee, *Int. J. Thermophys.* **17**:803 (1996).
21. S. L. Outcalt and M. O. McLinden, *Int. J. Thermophys.* **16**:79 (1995).
22. L. A. Weber and A. R. H. Goodwin, *J. Chem. Eng. Data* **38**:254 (1993).
23. P. F. Malbrunot, P. A. Meunier, G. M. Scatena, W. H. Mears, K. P. Murphy, and J. V. Sinka, *J. Chem. Eng. Data* **13**:16 (1968).
24. A. Kanungo, T. Oi, A. Popowicz, and T. Ishida, *J. Phys. Chem.* **91**:4198 (1987).
25. H. Russell, D. R. V. Golding, and D. M. Yost, *J. Am. Chem. Soc.* **66**:16 (1944).
26. S. L. Outcalt, personal communication (NIST, Thermophysics Division, Boulder, CO, 1995).
27. A. R. H. Goodwin D. R. Defibaugh, and L. A. Weber, *Int. J. Thermophys.* **13**:837 (1992).
28. J. W. Magee and J. B. Howley, *Int J. Refrig.* **15**:362 (1992).
29. M. Türk, J. Zhai, M. Nagel, and K. Bier, *Messung des Dampfdruckes und der kritischen Zustandsgrößen von neuen Kältemitteln*, Fortschrittberichte VDI Reihe 19, No. 79 (VDI-Verlag, Düsseldorf, 1994).
30. R. Tillner-Roth, *Int. J. Thermophys.* **16**:91 (1995).
31. J. W. Magee, personal communication (NIST, Thermophysics Division, Boulder, CO, 1995).

32. C. S. Cragoe, C. H. Meyers, and C. S. Taylor, *J. Am. Chem. Soc.* **42**:206 (1920).
33. N. S. Osborne and M. S. Van Dusen, *Sci. Pap. Bur. Stands.* **14**:439 (1917).
34. S. J. Boyes and L. A. Weber, *Int. J. Thermophys.* **15**:443 (1994).
35. B. A. Younglove, personal communication (NIST, Thermophysics Division, Boulder, CO, 1995).
36. A. R. H. Goodwin, D. R. Defibaugh, G. Morrison, and L. A. Weber, *Int. J. Thermophys.* **13**:999 (1992).
37. B. A. Younglove and M. O. McLinden, *J. Phys. Chem. Ref. Data* **23**:731 (1994).
38. L. Haar and J. S. Gallagher, *J. Phys. Chem. Ref. Data* **7**:635 (1978).
39. J. W. Magee, *Int. J. Refrig.* **15**:372 (1992).